Journal of
Functional Biomaterials

MDPI

Article

Calcium Hydroxide-Loaded Chitosan/Gelatin Nanocarriers: Physicochemical Characterization and In Vitro Antibiofilm Activity Against *Fusobacterium Nucleatum*

Maha Alghofaily [1,*], Abdulrahman Al-Majed [1], Basmah M. Almaarik [2], Manikandan Muthurangan [3], Sameerah Shaheen [3], Eram Eltahir [4], Fadilah Sfouq Aleanizy [4] and Fulwah Yahya Alqahtani [4]

1 Restorative Dental Sciences, College of Dentistry, King Saud University, Riyadh 11545, Saudi Arabia; aalmajed.96@gmail.com
2 Department of Clinical Laboratories, College of Applied Medical Sciences, King Saud University, Riyadh 12372, Saudi Arabia; balmaarik@ksu.edu.sa
3 Department of Anatomy and Stem Cell Unit, College of Medicine, King Saud University, Riyadh 11451, Saudi Arabia; mrangan@ksu.edu.sa (M.M.); sshahee@ksu.edu.sa (S.S.)
4 Department of Pharmaceutics, College of Pharmacy, King Saud University, Riyadh 11451, Saudi Arabia; ekeltahir@ksu.edu.sa (E.E.); faleanizy@ksu.edu.sa (F.S.A.); fyalqahtani@ksu.edu.sa (F.Y.A.)
* Correspondence: malghofaily@ksu.edu.sa

Abstract

Chronic microbial infection is a significant contributor to endodontic therapy failure, particularly when anaerobic organisms such as *Fusobacterium nucleatum* (*F. nucleatum*) are involved. Calcium hydroxide (Ca $(OH)_2$; CH) is a conventional intracanal medicament; however, its limited solubility, rapid washout, and lack of sustained release may limit its effectiveness. This study aimed to evaluate the in vitro antibacterial and antibiofilm activity of a CH-loaded chitosan/gelatin (CS/GEL) nanocarrier (NC) against *F. nucleatum*. CH-loaded CS/GEL NCs were prepared and characterized in terms of particle size, polydispersity index, zeta potential, and encapsulation efficiency. Fourier transform infrared spectroscopy and differential scanning calorimetry were used for further NC characterization. Antibiofilm activity was evaluated using crystal violet staining, confocal laser scanning microscopy (CLSM), and scanning electron microscopy (SEM). CH-loaded CS/GEL NCs exhibited a mean particle size of 423.2 nm (blank carrier, 372.5 nm), a low polydispersity index of 0.284 (indicating homogeneity), a zeta potential of +22 mV, and encapsulation efficiency of 98.46%. Fourier transform infrared spectroscopy and differential scanning calorimetry findings supported the incorporation of CH into CS/GEL NCs. In vitro release indicated sustained CH release over approximately 250 h. CH-loaded CS/GEL NCs produced lower biofilm biomass and a higher proportion of membrane-compromised bacteria in single-species biofilms of *F. nucleatum* on human radicular dentin than conventional CH paste at Day 14.

Keywords: calcium hydroxide; chitosan; gelatin; *Fusobacterium nucleatum*; intracanal medicament; biofilm

Check for updates

Academic Editors: Miriam Di Martino and Simona Concilio

Received: 30 October 2026
Revised: 22 November 2026
Accepted: 24 November 2026
Published: 28 November 2026

Copyright: © 2026 by the authors. Licensee MDPI, Basel, Switzerland. This article is an open access article distributed under the terms and conditions of the Creative Commons Attribution (CC BY) license.

1. Introduction

The primary objective of nonsurgical endodontic therapy is the thorough elimination of microorganisms from the root-canal system [1]. Failure to eradicate microorganisms, particularly those inhabiting the intricate structure of dentinal tubules and lateral canals, is the primary cause of post-treatment endodontic disease [2]. Given the polymicrobial

nature of apical periodontitis, effective disinfection requires thorough mechanical cleaning, chemical irrigation, and the use of an intracanal medicament (ICM) [2].

The Gram-negative anaerobic rod, *Fusobacterium nucleatum* (*F. nucleatum*), is a significant contributor to endodontic infections [3,4]. As a pivotal "bridge organism," it readily co-aggregates with both early and late colonizers, thereby promoting treatment-resistant biofilm formation [4]. Therefore, effective ICM should provide robust and sustained activity against *F. nucleatum*.

Calcium hydroxide ($Ca(OH)_2$; CH) is the gold-standard ICM in dentistry, primarily owing to its elevated alkalinity (approximately pH = 12.5), which disrupts bacterial-cell membranes and impairs enzymatic function [5]. However, its effectiveness as an ICM is limited by the challenging root-canal milieu [6] CH pastes exhibit limited solubility, fast disintegration, and rapid washout into the periapical tissues or via dentinal fluid, leading to a short therapeutic release time and often necessitating multiple clinical visits to achieve sufficient bacterial reductio [6].

To address these limitations and achieve a sustained-release CH profile, increasing attention has been given to biodegradable polymeric delivery systems [7]. Chitosan (CS), a natural linear polysaccharide, and gelatin (GEL), a denatured collagen protein, are attractive biomaterials owing to their superior biocompatibility, biodegradability, and ability to form stable hydrogels and scaffolds [8–10]. CS/GEL composites provide a favorable matrix for the encapsulation of CH, potentially extending its release kinetics and improving its therapeutic efficacy within the root-canal environment. Farhadian et al. (2018) developed and optimized CH-encapsulated CS/GEL nanocarriers and assessed the release of calcium ions [9]. However, their work was limited to physicochemical characterization and ion release kinetics. It is unclear whether the sustained release translates into biological benefit, specifically whether CH-loaded CS/GEL NCs can eliminate established endodontic pathogen biofilms over time, how they perform in comparison to commercially available CH pastes, and whether they are compatible with the periapical host cells with which they are likely to interact [9]. These inquiries are crucial for evaluating the formulation's capability for CH delivery in endodontic uses.

F. nucleatum is highly virulent and shows notable resistance to commonly used irrigants and ICM [11], which helps it persist in root canal infections. Despite this, the susceptibility of *F. nucleatums* biofilms to novel CH delivery systems has not been investigated. Therefore, the present research aimed to (i) evaluate the antibiofilm activity of CH-loaded CS/GEL NCs against *F. nucleatum* at 7 and 14 days, using crystal violet biomass quantification and confocal live/dead imaging, and compare this activity with that of a conventional CH paste (UltraCal) and of empty CS/GEL NCs to distinguish the contribution of the carrier from that of the encapsulated CH, and to (ii) assess the cytocompatibility of the formulation toward hBMSCs.

2. Materials and Methods

2.1. Materials

Low-molecular-weight CS (50–190 kDa; degree of deacetylation [DD] = 75–85%), GEL, and CH were purchased from Sigma-Aldrich (Burlington, MA, USA).

2.2. Preparation of the CH-Loaded CS/GEL NC System

The CS/GEL NC system was prepared using a previously described method with minor modifications [9]. A low-molecular-weight CS solution was prepared at a concentration of 0.1% (w/v) in 1% (v/v) acetic acid to obtain a transparent solution. Tween 80 non-ionic surfactants were added at a concentration of 1.0% (w/v). The pH of the CS solution was adjusted to 4.8 using 10 N sodium hydroxide (NaOH). GEL solutions were prepared by

dissolving different GEL concentrations (0.3–5% *w*/*v*) in phosphate-buffered solution (pH: 5) under simultaneous heating and stirring. A calcium hydroxide solution was prepared by dissolving an appropriate amount of CH powder in distilled water to obtain 0.36% *w*/*v*.

Different formulations were prepared by first adding the GEL solution to the CS solution and mixing using a probe sonicator. CH solution was then added dropwise to the CS/GEL solution under the same condition. Following addition of CH, the NCs formed spontaneously under probe sonication for 2 min 15 s. The resultant NCs were stored until further analysis.

2.3. Characterization of Prepared Nanoparticles

Particle size, polydispersity index (PDI), and zeta potential (ZP) were measured using dynamic light scattering with a Zeta sizer (Particle Sizing Systems, Port Richey, FL, USA). All measurements were performed in triplicate.

2.4. Determination of Encapsulation Efficiency of the CH-Loaded CS/GEL NCs

The encapsulation efficiency (EE) of CH in the NCs was estimated by quantifying calcium ions. Briefly, 1 g of the formulation was dissolved in 50 mL of 1 M NaOH, and 1 mL of this solution was further diluted in 10 mL of 1 M NaOH. Calcium ion concentration was determined using a Calcium Arsenazo III kit (Linear Chemicals, Barcelona, Spain). The assay is based on the specific complexation of calcium ions (Ca^{2+}) with Arsenazo III under mildly acidic conditions (pH 6.5), resulting in the formation of a blue-purple calcium–Arsenazo III complex. The intensity of the resulting color is directly proportional to the calcium concentration in the sample and is quantified using a UV–visible spectrophotometer (Biochrom Libra S22, Biochrom Ltd., Cambridge, UK) at 650 nm. The measured calcium concentration was used to calculate the calcium content of the formulation after accounting for the dilution factor. Absorbance was measured using spectrophotometry at a wavelength of 650 nm (Biochrom Libra S22 UV/Vis spectrophotometer; Biochrom Ltd., Cambridge, UK). Drug content was calculated as follows:

$$\text{Drug content} = (\text{Concentration} \times \text{Dilution factor} \times \text{Volume taken}) \times \text{Conversion factor}$$

The EE% of the formulation was calculated as follows:

$$\text{EE}\,\% \;= \%\left(\frac{W_D}{W_T}\right) \times 100$$

where W_D = weight of CH in NCs and W_T = weight of initial CH.

2.5. Differential Scanning Calorimetry (DSC) Analysis

The DSC experiments were performed using DSC4000 (PerkinElmer, Shelton, CT, USA) in nitrogen at a 20 mL/min flux rate and at a temperature range of 30–400 °C with a 10 °C heating rate per min. Samples (5–6 mg) were placed in covered aluminum pans, sealed and compressed, with the empty pan used as the reference sample.

2.6. Chemical Characterization by Fourier Transform Infrared (FTIR) Spectroscopy

FTIR analysis was performed using an IRAffinity-1S spectrometer (Shimadzu Corp., Kyoto, Japan). Powdered samples (60 mg) were mixed with 100 mg of potassium bromide, compressed into tablets, and analyzed over the range of 4000–400 cm^{-1} at a resolution of 4 cm^{-1}.

2.7. In Vitro Release Assay

A specified volume of CH-loaded NC suspension from each sample was placed in a 25 mL centrifuge tube containing phosphate-buffered saline (PBS; Gibco, Thermo

Fisher Scientific, Waltham, MA, USA) and placed in a dialysis bag. The dialysis bag was submerged in a glass container containing phosphate buffer (pH 7.4) and placed on electronic shaker operating at 100 rpm and 37 °C. At predetermined time points, 1 mL of the supernatant was withdrawn for analysis, and an equal volume of fresh PBS was added. Calcium ion concentration was quantified using an ultraviolet spectrophotometer, as described above.

2.8. Anti-Biofilm Effect of CH as an ICM Against F. Nucleatum in Human Tooth Model

Institutional approval (IRB number: E-24-9022) was obtained to prepare human radicular dentin disks (4 × 4 × 1 mm). Disks were treated with 17% ethylenediaminetetraacetic acid for 1 min using ultrasonic agitation, then rinsed and autoclaved at 121 °C for 1 h. *F. nucleatum* (ATCC 10953; American Type Culture Collection, Manassas, VA, USA) was grown anaerobically at 37 °C, adjusted to an optical density of 600 nm = 0.5, and inoculated into dentin disks (1 mL per well). Biofilms were allowed to grow for 72 h under anaerobic conditions [12].

The experimental groups were (1) empty CS/GEL, (2) CH-loaded CS/GEL, and (3) CH paste (UltraCal; Ultradent Products, South Jordan, UT, USA). Infected dentin disks treated with saline were used as the positive control, while sterilized dentin disks served as the negative control. Following the establishment of the biofilm, the culture media were exchanged for 0.5 mL of broth and 0.5 mL of the specified therapeutic agent. The specimens were then incubated in anaerobic conditions for 7 or 14 days.

The quantification of biofilm biomass was performed through a crystal violet assay based on O'Toole's adaptation [13], measuring absorbance at 595 nm. For confocal viability analysis, specimens were stained with SYTO 9 and propidium iodide before being imaged with confocal laser scanning microscopy (CLSM). ImageJ software version 1.54J (National Institutes of Health, Bethesda, MD, USA) was used to calculate the red fluorescence ratio (red/[red + green]), which represents the percentage of dead bacteria. SYTO 9/propidium iodide staining reports bacterial membrane integrity only. The carriers were not fluorescently labelled; therefore, CLSM was not used to localize the carriers or to assess their penetration into the biofilm or dentinal tubules. After a period of seven days of intervention, samples from all groups were observed using a JEOL® JSM-6610LV Scanning Electron Microscope (JEOL, Tokyo, Japan).

2.9. Cell Culture and Viability

To assess the biocompatibility of the CH-loaded formulation, a telomerized human bone marrow mesenchymal stem cell (hBMSC) line (hMSC-TERT) was used.

This cell line was sourced from the stem cell unit of the anatomy department at King Saud University's College of Medicine and was developed via the overexpression of the human telomerase reverse transcriptase gene (hTERT) [14,15]. Cells were grown in Dulbecco's Modified Eagle Medium (DMEM) supplemented with D-glucose (4500 mg/L), 4 mM of L-glutamine, 110 mg/L of sodium pyruvate, 10% fetal bovine serum (FBS), 1× penicillin-streptomycin (Pen-strep), and nonessential amino acids (all purchased from Gibco, Thermo Fisher Scientific, Waltham, MA, USA) and maintained in a humidified atmosphere of 5% CO_2 at 37 °C.

We tested the formulations across a range of concentrations (C1–C6) (supplementary). The concentration used in the viability assay (C4) was the same as that used in the antibacterial and antibiofilm experiments, so that cytocompatibility was evaluated at the concentration that showed antibacterial efficacy. Untreated cells in culture medium (DMEM) served as the control. In brief, cells were introduced into 24-well plates (1×10^6 cells/well) and incubated for 24 h for attachment. Then, 0.5 mL from each assigned experimental group

was added to 0.5 mL of medium and incubated. After 2 days of incubation, the AlamarBlue assay (AbD Serotec, Kidlington, UK) measured cell viability. Then, 10% AlamarBlue was added to each well and incubated for 2 h. The fluorescence in each well was measured at 590 nm with excitation at 530 nm using a fluorescence reader (BioTek, Winooski, VT, USA). Cell viability was expressed as a percentage of the untreated control, and values above 70% were considered non-cytotoxic according to ISO 10993-5:2009) [16]. All experiments were carried out in triplicate, with three wells per condition.

2.10. Statistical Analysis

The Shapiro–Wilk test was utilized to evaluate normality. A two-way factorial analysis of variance (ANOVA) was used to investigate the effects of group, time, and interaction on antibiofilm outcomes, as well as group, concentration, and interaction effects on cytotoxicity. All inferential statistical analyses were performed at a significance level of 0.05. p-values < 0.05 were considered statistically significant. Statistical analyses were carried out with IBM SPSS Statistics, version 30 (IBM Corp., Armonk, NY, USA).

3. Results

3.1. Properties of Formulated CH-Loaded CS/GEL NCs

CS/GEL NCs were successfully formulated. As demonstrated in Table 1, the particle sizes of the produced NCs were 372.5 nm and 423.2 nm for empty CS/GEL NCs and CH-loaded CS/GEL NCs, respectively. The PDI increased only slightly from 0.235 for empty CS/GEL NCs to 0.284 following CH loading, indicating homogeneity. Similarly, the ZP increased in the loaded formula to 22 mV when compared with that of the empty nanoparticles, which was 17.13 mV. The encapsulation efficiency of CH in NC was 98.46% (Table 1).

Table 1. Characteristics of empty CS/GEL NCs and CH-loaded CS/GEL NCs.

Formula	PS (nm ± SD)	PDI ± SD	ZP (mV ± SD)	EE% ± SD
Empty CS/GEL NC	372.5 ± 0.90	0.235 ± 0.014	17.13 ± 0.56	-
CH-loaded CS/GEL NC	423.2 ± 2.36	0.284 ± 0.027	22 ± 0.173	98.46 ± 0.57

PS, PDI, ZP, and EE% of produced NCs were evaluated. Results are shown as mean ± SD, $n = 3$. CS, chitosan; GEL, gelatin; NC, nanocarrier; CH, calcium hydroxide; PS, particle size; PDI, polydispersity index; ZP, zeta potential; EE, encapsulation efficiency; SD, standard deviation.

3.2. Thermal Characterization by Differential Scanning Calorimetry (DSC)

DSC was used to evaluate the thermal behavior of the samples and assess the incorporation of CH within the CS/GEL NC system. Pure CS (B) showed an exothermic peak at around 300–320 °C linked to polymer breakdown after a wide endothermic transition at about 80–100 °C caused by the evaporation of absorbed and bound water. Similar to this, GEL (C) showed a wide endothermic transition between 80 and 100 °C as a result of moisture loss; transitions at higher temperatures could be the result of structural alterations and thermal protein matrix disintegration. Distinct variations in the thermal transitions of the empty CS/GEL (D) and the CH-loaded CS/GEL (E) confirmed successful encapsulation. The endothermic peak shifted from 68.96 °C in the empty CS/GEL to 88.13 °C in the CH-loaded CS/GEL (Figure 1D,E). This approximately 19 °C shift in the endothermic peak may reflect interactions between CH and the polymer matrix, possibly through hydrogen bonding or structural stabilization. A slight increase in enthalpy (ΔH) was also observed, from 167.72 J/g in the empty CS/GEL to 169.42 J/g in the CH-loaded CS/GEL,

indicating a change in energy absorption upon CH incorporation. In contrast, the DSC spectrum of pure CH (Figure 1A) exhibited peaks at 112.90 °C and 339.39 °C, which were not distinctly observed in the CH-loaded CS/GEL, indicating successful encapsulation of CH within the NC. The absence of these peaks and broadening of the thermal transitions further support the encapsulation of CH within the CS/GEL NCs. Overall, CH loading altered the thermal properties of the NC system, resulting in improved thermal stability and phase-transition behavior.

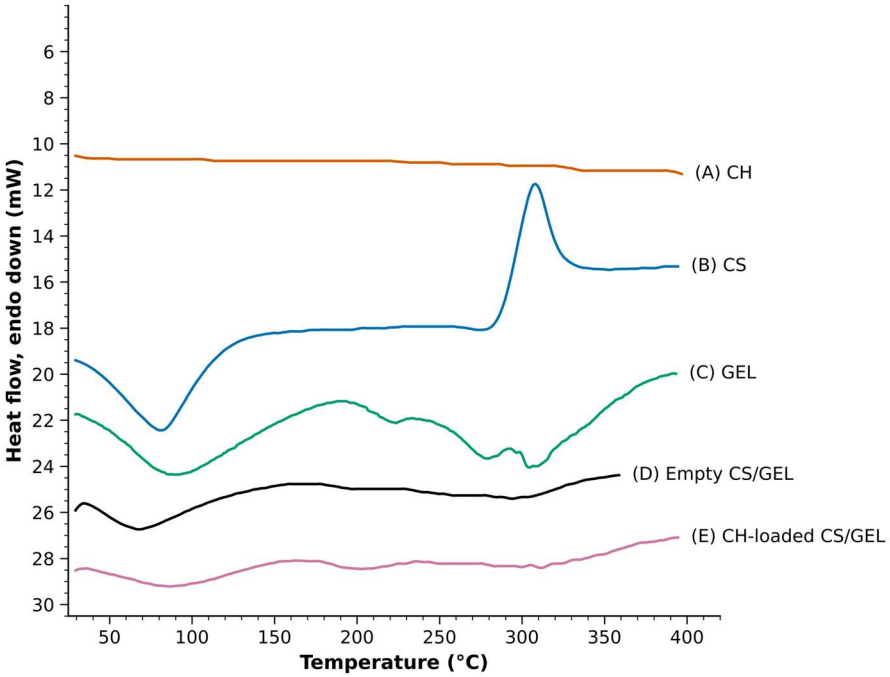


Figure 1. DSC thermograms of (A) CH, (B) CS, (C) GEL, (D) empty CS/GEL, and (E) CH-loaded CS/GEL, recorded from ~30 to 400 °C. Endothermic events point downward. (DSC, differential scanning calorimetry; CH, calcium hydroxide; CS, chitosan; GEL, gelatin.).

3.3. Fourier Transform Infrared (FTIR) Spectroscopy

FTIR analysis was performed to evaluate the incorporation of CH into the CS/GEL NCs (Figure 2). FTIR analysis showed that both the empty CS/GEL nanocarrier and the CH-loaded formulation retained the principal distinctive polymer bands, with signals around 1647, 1560, 1508, and 1448 cm^{-1}. In the CH-loaded nanocarrier (Sample E), spectral alterations were observed in the carbonyl and fingerprint domains, with the band around 1701 cm^{-1} in the blank carrier changing to 1724 cm^{-1} and the band at 1356 cm^{-1} moving to 1341 cm^{-1}.

Calcium hydroxide alone exhibited a pronounced hydroxyl absorption at about 3640 cm^{-1}; yet this distinctive band was not clearly identified as a separate peak in the loaded nanocarrier. Consequently, the FTIR results suggest alterations in the chemical interactions of the CS/GEL matrix after the incorporation of CH, aligning with the physicochemical interactions between calcium hydroxide and the nanocarrier.

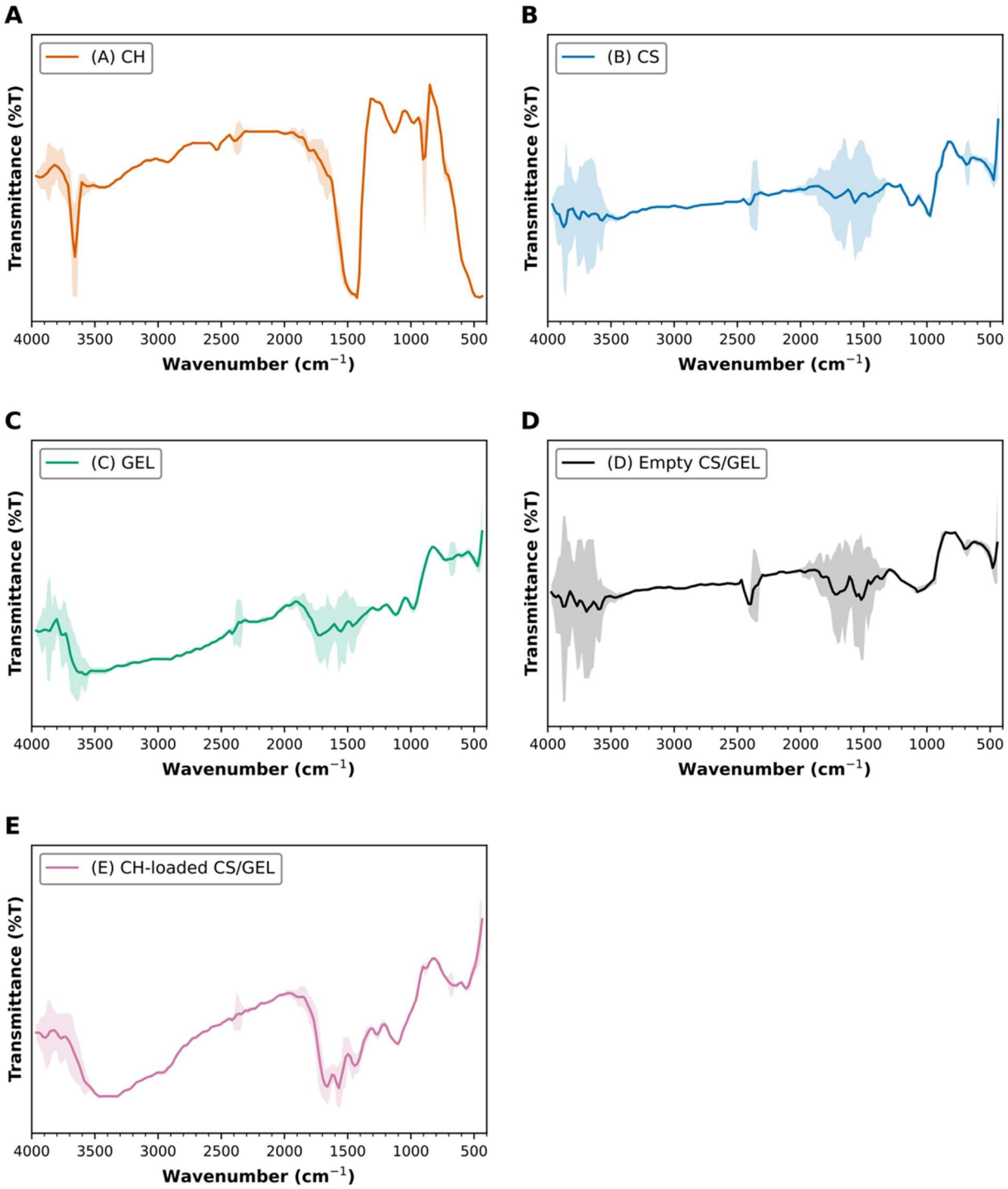


Figure 2. FTIR spectra of (**A**) CH, (**B**) CS, (**C**) GEL, (**D**) empty CS/GEL, and (**E**) CH-loaded CS/GEL (4000–400 cm^{-1}). (FTIR, Fourier-transform infrared spectroscopy; CH, calcium hydroxide; CS, chitosan; GEL, gelatin.).

3.4. In Vitro Release Study

The release study demonstrated that 100% of the CH was released within approximately 250 h (Figure 3) compared with 70% of CH released within 400 h in previous research [9]. This difference may be related to the DD of the CS used. The CS in a previous study [9] had a DD of 91%, compared with 75–85% DD in the current study. Lower DD results in fewer free amino groups (-NH_2) and weakens hydrogen bonding with GEL [17,18]. This results in a less cohesive polymeric matrix, allowing faster CH diffusion and release [17,18].

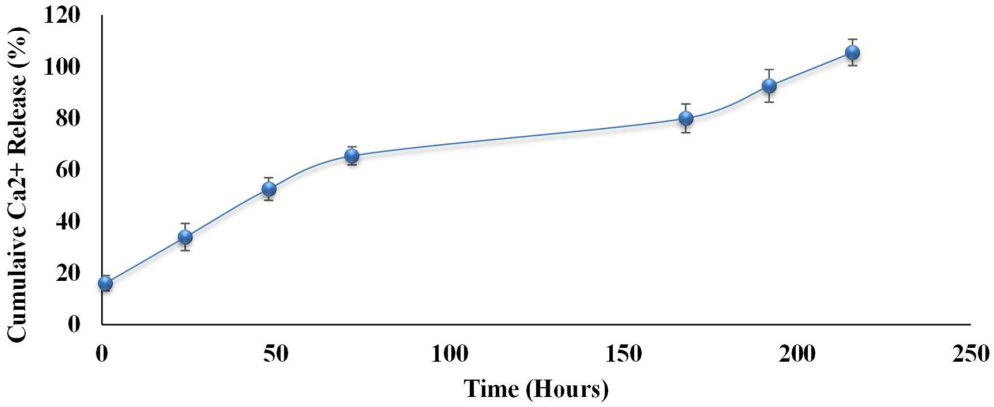


Figure 3. Cumulative in vitro release of Ca^{2+} from CH-loaded CS/GEL NCs in phosphate buffer (pH 7.4, 37 °C, 100 rpm). Data are shown as mean ± SD ($n = 3$). (CH, calcium hydroxide; CS, chitosan; GEL, gelatin; NC, nanocarrier.).

3.5. Biofilm Mass Analysis

Biofilm biomass was quantified using the crystal violet assay ((Table 2). Table 2 presents these data by group and time point, with post hoc comparisons. Two-way factorial ANOVA was used to examine the effect of time, group and time × group interaction. All three were found statistically significant (all $p < 0.001$) with large effect sizes (time $\eta^2 = 0.94$, group $\eta^2 = 0.99$, interaction $\eta^2 = 0.96$). Overall statistics were as follows: Time $F(1,16) = 237.74$, $p < 0.001$; Group $F(3,16) = 480.89$, $p < 0.001$; Interaction $F(3,16) = 123.31$, $p < 0.001$. Significant time increase overall was found between day 7 (M = 1.14) and day 14 (M = 1.86), $p < 0.001$. With regard to groups, all pairwise differences are statistically significant ($p \leq 0.012$). Significant interaction suggests that change over time differs between groups.

Table 2. Biofilm biomass (crystal violet OD595) by group and time point, with simple main effects and post hoc comparisons.

Group	Day 7	Day 14	Change Over Time (Day 7 vs. 14)
Empty CS/GEL	0.66 ± 0.004 ^{b}	2.88 ± 0.21 ^{a}	$F(1,16) = 570.29$, $p < 0.001$
CH-loaded CS/GEL	0.60 ± 0.001 ^{b}	0.55 ± 0.06 ^{c}	$F(1,16) = 0.30$, $p = 0.590$
CH paste (UltraCal)	0.74 ± 0.17 ^{b}	0.90 ± 0.05 ^{b}	$F(1,16) = 2.70$, $p = 0.120$
Saline (untreated)	2.55 ± 0.13 ^{a}	3.10 ± 0.08 ^{a}	$F(1,16) = 34.37$, $p < 0.001$
Difference between groups	$F(3,16) = 204.53$, $p < 0.001$	$F(3,16) = 399.66$, $p < 0.001$	

Note: Values are mean ± SD ($n = 3$ per group per day). Two-way ANOVA: time $F(1,16) = 237.74$, group $F(3,16) = 480.89$, time × group $F(3,16) = 123.31$ (all $p < 0.001$; partial $\eta^2 = 0.94, 0.99, 0.96$). Superscript letters denote Bonferroni-adjusted pairwise comparisons among groups on the same day (a = highest mean); groups sharing a letter within a column do not differ statistically. Day 14: CH-loaded CS/GEL vs. CH paste, $p = 0.011$; empty CS/GEL vs. saline, $p = 0.213$; all other pairs, $p < 0.001$. Day 7: Empty CS/GEL, CH-loaded CS/GEL and CH paste did not differ from one another ($p = 0.88$ to 1.00); each differed from saline ($p < 0.001$). The last column shows the simple main effect of time within each group (shaded, $p < 0.05$).

3.6. Biofilm Viability Analysis

Live/dead fluorescent staining followed by CLSM was used to quantify *F. nucleatum* viability (Figure 4A). Image-based analysis quantified the percentage of dead bacteria as the ratio of red fluorescence to total fluorescence (red + green). These findings were consistent with the biomass analysis. The CH-loaded CS/GEL group showed the highest proportion of dead (propidium iodide-positive) bacteria at both time points (79.7% at Day 7 and 65.7% at Day 14), followed by CH paste (51.0% and 55.3%), empty CS/GEL (47.0% and 29.3%), and saline (15.7% and 12.7%) (Figure 4B). Because propidium iodide uptake reflects

membrane damage rather than loss of culturability, these values indicate the proportion of membrane-compromised cells and are not a direct measure of bacterial killing.

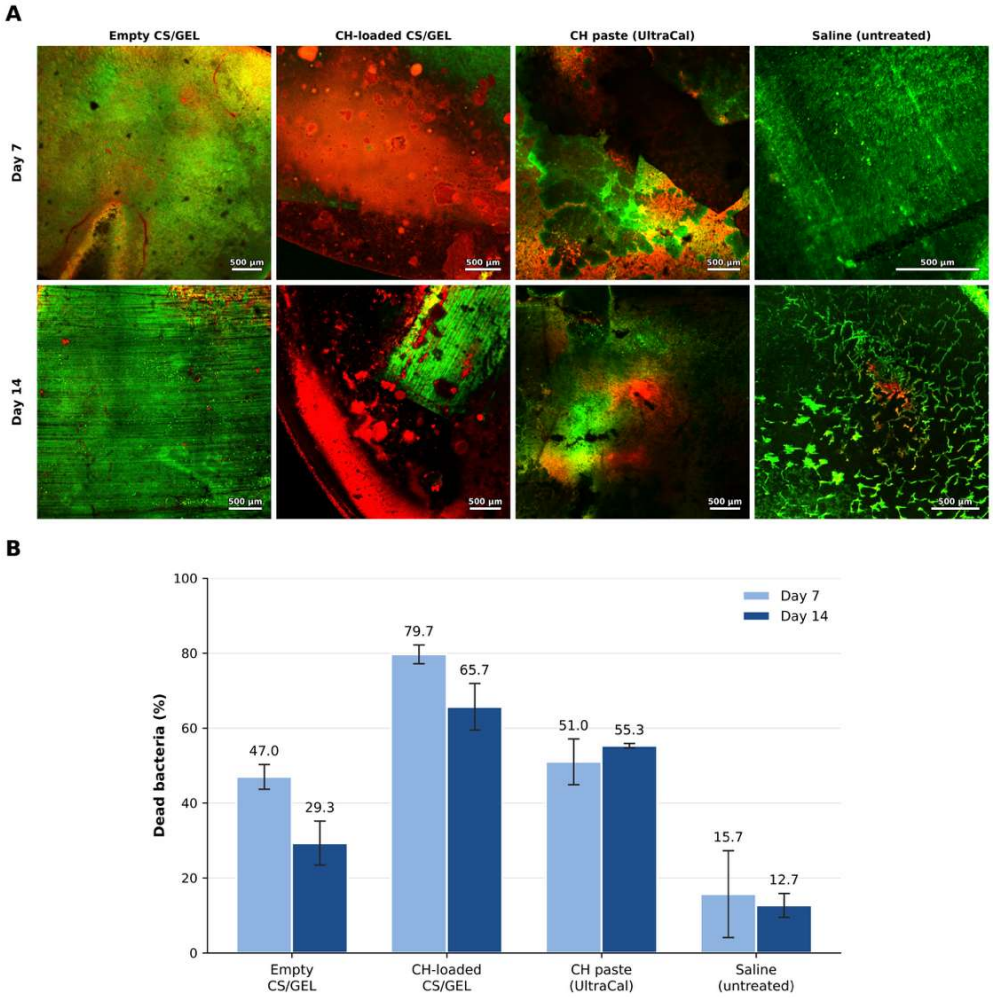


Figure 4. Dentine biofilm viability analysis. (**A**) Representative fluorescence images of *Fusobacterium nucleatum* biofilm cells stained with a live/dead assay (green = live cells; red = dead cells). (**B**) Mean percentage of dead bacteria at Days 7 and 14 across all experimental groups. The percentage of dead bacteria was calculated as red/(red + green) fluorescence and reflects membrane integrity, not viable counts.

3.7. Morphological Assessment of Biofilm Formation

The morphology of the formed biofilms was examined using scanning electron microscopy to assess bacterial adhesion and structural organization (Figure 5). Images shown are representative of five independent images acquired for each treatment type.

At ×500, the untreated saline control showed a dense, continuous layer covering the dentin surface. In both CS/GEL groups, the surface was covered by a fibrous, web-like network, most likely polymer residue from the carrier; in the CH-loaded CS/GEL group, this network converged on aggregates of deposits. The CH paste group showed a granular surface of crystalline deposits rather than a continuous biofilm layer. At this magnification, individual bacterial cells cannot be reliably distinguished from polymer fibres or mineral deposits. The SEM images are therefore presented as a qualitative description of surface coverage and were not used to assess bacterial morphology or viability.

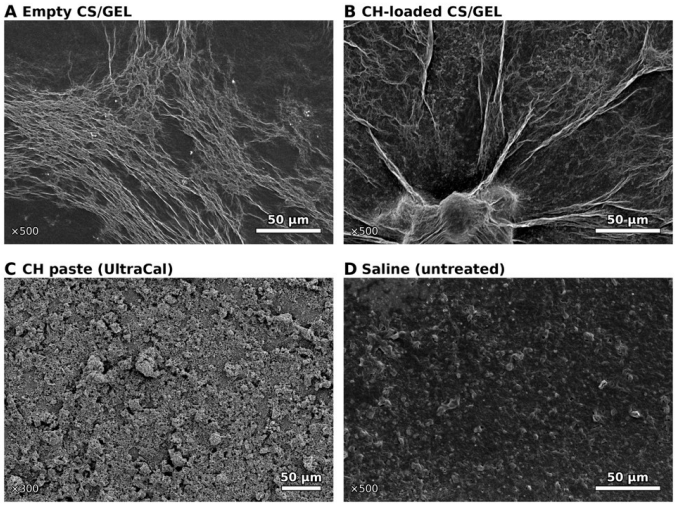


Figure 5. Representative scanning electron microscopy images of *Fusobacterium nucleatum* showing bacterial adhesion and biofilm formation after 7 days of treatment. Magnification, ×500; scale bars = 50 µm.

3.8. AlamarBlu Cell Viability Assay

To characterize the dose-dependence of cytotoxicity, six concentrations (C1 (2.5 mg) to C 6 (0.0781 mg)) of loaded nanocarriers were prepared. Then, C4 (0.3125 mg) was selected. The concentration used is comparable to that used in the antibacterial experiments (35% CH), which is also the highest dose before the fluorescence signal fell for the CH-loaded nanocarriers. Fluorescence did not differ significantly between the selected concentration (0.3125 mg; 1728 fluorescence units) and the lowest concentration (0.0781 mg; 1851), but fell to 1309 at 0.625 mg (Supplementary Table S1).

The hBMSC viability was 75.9 ± 0.6% with the CH-loaded CS/GEL, comparable to the empty CS/GEL NCs (76.3 ± 0.7%), and was markedly higher than that with the CH paste (4.3 ± 0.1%; $p < 0.001$) (Figure 6).

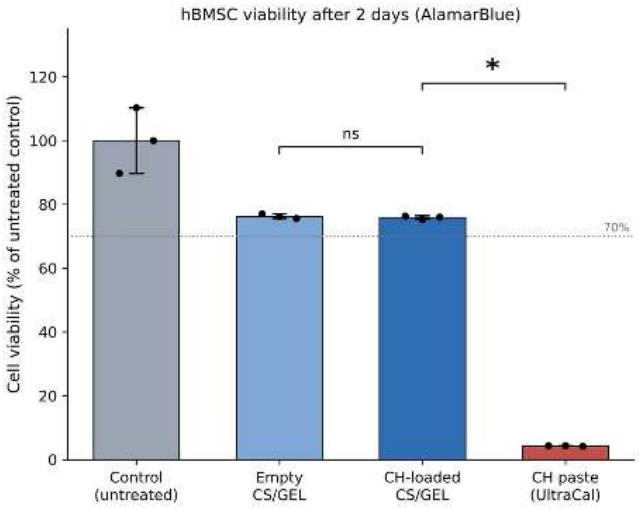


Figure 6. hBMSC viability after 2 days of exposure to empty CS/GEL NCs, CH-loaded CS/GEL NCs, and conventional CH paste (UltraCal), measured with the AlamarBlue assay and expressed as a percentage of the untreated control (mean ± SD, $n = 3$; dots show individual replicates). The dotted line marks the 70% cytocompatibility threshold (ISO 10993-5). ns, not significant; * $p < 0.001$, CH-loaded CS/GEL vs. CH paste.

4. Discussion

The in vitro results of the current study indicate that CH can be integrated into CS-based NCs with physicochemical properties conducive to loading and delivery. The empty CS/GEL NCs exhibited a particle size of 372.5 nm, whereas the CH-loaded CS/GEL NCs had a larger particle size of 423.2 nm. Loading resulted in a slight increase in PDI from 0.235 to 0.284 and in ZP from 17.13 mV to 22 mV.

The distinct methods by which ionic gelation compacts CS chains and composite CS/GEL networks incorporate inorganic species may be the reason for the smaller size of empty NCs compared to CH-loaded NCs [9]. Formulation variables like ionic strength can affect particle size, PDI, and ZP, but ionic gelation can produce uniform particles [19]. In contrast, adding CH to CS/GEL systems may increase assembly size and hydration [20]. The present study employed sonication-assisted mixing of CS and GEL solutions to incorporate CH, which was subsequently added dropwise during sonication. This process enabled the formation of NC in situ; 98.46% CH EE was achieved with this method.

The in vitro release study showed that 100% of the CH was released within approximately 250 h, indicating a controlled-release therapeutic profile. This entrapped CH must first dissolve into Ca^{2+} and OH^{-} ions and then diffuse through the hydrated chitosan–gelatin network before reaching the release medium. Consistent with this mechanism, total calcium release from the CH-loaded CS/GEL nanocarriers reached almost 100% after 250 h. Release behavior may be controlled by hydration and swelling of hydrophilic CS/GEL matrix, followed by dissolution of CH and diffusion of calcium ions via the polymeric network. Release may also be aided by matrix relaxation and progressive degradation. Degree of deacetylation of CS, polymer composition and intermolecular interactions may determine matrix permeability and release kinetics. This may be partially explained by the lower degree of deacetylation utilized in the current work (75–85%) compared to the previously reported formulation using CS with a degree of deacetylation of 91%. However, this association has to be experimentally confirmed. The measured trend consequently indicates extended calcium release, but the proportional roles of diffusion, swelling and polymer erosion have to be determined. Roig et al. assessed the release behavior of CH when it was dispersed within a thermosensitive gel intended for intracanal application and incorporated into nanoparticles [19]. The release pattern of free CH is typically characterized by an initial rapid-release phase followed by a slower, sustained release, with maximum release occurring after approximately 250 h. In the study by Roig et al., free CH exhibited a faster release pattern, characterized by an early burst followed by a slow decline, with peak release in approximately 150 h [19].

In addition to potentially improving therapy efficacy and reducing the need for repeated administration, sustained release may also assist in maintaining therapeutic medication concentrations over an extended period, thereby improving patient adherence and treatment convenience. Keeping medication concentrations consistent can reduce the risk of adverse effects from abrupt drug exposure [21].

We found that both CH-containing formulations reduced the biofilm biomass of *F. nucleatum* on dentin compared with saline over the 2-week study period. Crystal violet testing demonstrated that CH-loaded CS/GEL NCs showed one of the lowest biomass values at Day 7 (0.60 ± 0.001) and remained low at Day 14 (0.55 ± 0.06), whereas empty CS/GEL NCs showed a marked increase in biomass by Day 14 (2.88 ± 0.21). CLSM live/dead analysis was consistent with this pattern: the CH-loaded CS/GEL group showed the highest proportion of membrane-compromised (propidium iodide-positive) bacteria at Day 14 (65.7%). This value means that approximately one-third of the bacterial signal still came from cells with intact membranes. It therefore indicates a partial reduction in the viable

biofilm rather than eradication, and because viable counts were not performed, it should not be interpreted as a direct measure of bacterial killing.

The transient antibacterial effect of empty CS/GEL NCs may be due to CS's low antimicrobial activity. CS nanoparticles may demonstrate a synergistic effect when combined with other antimicrobial agents, enabling deeper penetration of ICM into dentinal tubules and the neutralisation of bacterial surface charges [22]. CS alone has antimicrobial properties [23,24].

Each assay addresses a different aspect of the main comparison between CH-loaded CS/GEL and conventional CH paste. Crystal violet staining measures total adherent biomass, including cells and matrix; it does not distinguish live from dead bacteria and can also stain adsorbed polymer. CLSM live/dead staining reports the proportion of cells with compromised membranes but not their culturability. SEM provides a qualitative view of surface coverage, and the AlamarBlue assay addresses host–cell tolerance at a single concentration and exposure time. Three factors other than the delivery system itself may contribute to the differences observed. First, the CH content applied per specimen was not matched between the loaded formulation and the paste, so the comparison reflects formulation and dose together. Second, the blank carrier was not inert: at Day 7, empty CS/GEL reduced biomass to a level that did not differ from either CH-containing group (Table 2) and increased the proportion of dead bacteria relative to saline (Figure 4B), consistent with the intrinsic antimicrobial activity of CS noted above. Part of the effect of the loaded formulation may therefore derive from the carrier. The polymer deposits seen by SEM in the CS/GEL groups may also have contributed to crystal violet staining, particularly for the empty carrier at Day 14. Third, exposure time influenced the comparison: at Day 7, biomass did not differ among the three treated groups, and the CH-loaded formulation was superior to the paste only at Day 14. This is consistent with, but does not prove, a contribution of sustained CH release.

In our assay, the CH-loaded CS/GEL NCs demonstrated greater biofilm reduction and a higher proportion of membrane-compromised bacteria than conventional CH paste specifically after 14 days. Conventional CH pastes may exhibit limited penetration into tubules and established biofilms because of the buffering capacity of dentin [24]. Polymeric nanoparticle-based CH systems have been reported to increase the area of dentinal tubule penetration compared with free CH [25]. However, carrier penetration into the biofilm or dentinal tubules was not assessed in the present study, because the carriers were not labelled and SYTO 9/propidium iodide staining reports only bacterial membrane integrity. The higher proportion of dead bacteria observed with the CH-loaded system therefore cannot be attributed to this mechanism on the basis of our data. Similarly, pH at the biofilm–dentin interface was not measured, so maintenance of an alkaline microenvironment at this interface remains a hypothesis. Similar to previous endodontic formulations, CH has been integrated into CS/GEL NCs to optimize loading and extend the release of hydroxyl or calcium ions for intracanal use [9]. Gradual ion diffusion may assist in the preservation of an alkaline microenvironment at the biofilm dentin surface, whereas its incorporation into CS/GEL may influence biological responses and decrease CH solubility [26]. CH is dependent on hydroxyl-ion diffusion, which is easily buffered by dentin/biofilm [5].

Interestingly, loading CH into CS/GEL markedly reduced its cytotoxicity, addressing an important translational barrier for medications in regenerative endodontic procedures (REPs). Viability with both CS/GEL formulations remained above the 70% ISO 10993-5 threshold relative to untreated cells, indicating that, at the tested concentration (0.3125 mg) and a 2-day exposure, the cytotoxicity of the paste was largely avoided when CH was delivered in the carrier. These results suggest that NC incorporation may broaden the therapeutic window by reducing toxicity while maintaining antimicrobial activity, as predicted by the

concentration-dependent relationship. The cytotoxicity of calcium hydroxide is mainly attributed to the rapid release of hydroxyl ions and the resulting highly alkaline pH [5]. Loading CH into a chitosan/gelatin nanocarrier may moderate this effect by releasing it more gradually, which would limit peak alkaline exposure while keeping the antibacterial effect [20,27]. This is clinically relevant because intracanal medicaments can reach the periapical tissues through the apical foramen, lateral canals or accidental extrusion. There they contact mesenchymal stem cells that are essential to periapical healing and to regenerative endodontic procedures. A medicament that is antibacterial while preserving the viability of these cells would therefore be advantageous [28]. However, these findings come from a 2D monolayer model with direct exposure over 48 h. This model does not reproduce the buffering capacity of dentin, the confinement of the material within the root canal, or tissue clearance in vivo, and it may overestimate or underestimate cytotoxicity. Further studies with longer exposure times, other relevant cell types (e.g., SCAP and PDL fibroblasts) and in vivo models are needed to confirm that the formulation is safe for endodontic use. This balance is especially important in REPs, where effective disinfection must be achieved while preserving stem cell survival and regeneration potential. The central principle of REPs is to achieve effective antimicrobial disinfection without compromising apical stem-cell survival and regenerative potential [29]. Consistent with this principle, our findings showed that loaded formulations maintained markedly higher viability. Delivery systems that reduce cytotoxicity at higher nominal concentrations may widen the usable concentration window or achieve comparable antimicrobial effects with lower free-drug exposure. These observations apply only to the concentration, exposure time, and cell line tested and do not by themselves establish safety for clinical endodontic use.

Despite promising antibiofilm and cytocompatibility profiles, further research should examine whether NCs can maintain antibiofilm efficacy and reduce cytotoxicity in REP-realistic models. Polymicrobial biofilms and ex vivo infected teeth should be included in antimicrobial testing, which should also evaluate dentinal-tubule penetration and depth-resolved bacterial killing. In addition to the co-delivery of regenerative biomolecules, it is important to evaluate additional clinically relevant scenarios, including discoloration, interactions with ethylene-diaminetetraacetic acid-mediated growth-factor release, effects on dentin, and medicament removability. In particular, the present data were obtained in a single-species *F. nucleatum* biofilm model on dentin, and bacterial viability was inferred from live/dead staining without viable counts. Future work should include culture-based viable counts and confocal Z-stacks with orthogonal views and depth-resolved quantification of fluorescently labelled carriers, with free-dye and background controls, to test whether the carriers penetrate the biofilm and dentinal tubules.

5. Conclusions

Within the limitations of this in vitro, single-species dentin model, CH-loaded CS/GEL carriers produced lower *F. nucleatum* biofilm biomass and a higher proportion of membrane-compromised bacteria than conventional CH paste after 14 days and maintained hBMSC viability above 70% of the untreated control at the tested concentration after 2 days of exposure. These findings apply only to the doses and exposure conditions tested. Viable counts, multispecies biofilms, and ex vivo models are required before the antibacterial efficacy of the formulation and its suitability for endodontic use can be established.

Supplementary Materials: The following supporting information can be downloaded at: https://www.mdpi.com/article/10.3390/jfb17120624/s1, Table S1. Cytotoxicity analysis results.

Author Contributions: Conceptualization, M.A., A.A.-M. and F.Y.A.; Methodology, M.A., F.Y.A., B.M.A., F.S.A., M.M. and S.S.; Software, A.A.-M. and M.A.; Validation, M.A., F.Y.A., B.M.A., F.S.A.

and S.S.; Formal Analysis, A.A.-M., M.A., B.M.A., F.Y.A., F.S.A., E.E. and M.M.; Investigation, A.A.-M., M.A., B.M.A., F.Y.A., F.S.A. and E.E.; Resources, M.A., F.Y.A. and S.S.; Data Curation, M.A., A.A.-M., F.Y.A., B.M.A. and F.S.A.; Writing—Original Draft Preparation, M.A., A.A.-M., F.Y.A., F.S.A., B.M.A., E.E. and M.M.; Writing—Review & Editing, M.A., F.Y.A., F.S.A., B.M.A. and S.S.; Visualization, M.A., B.M.A., F.Y.A. and S.S.; Supervision, M.A.; Funding Acquisition, M.A. All authors have read and agreed to the published version of the manuscript.

Funding: This research was funded by the Ongoing Research Funding Program, King Saud University, Riyadh, Saudi Arabia, grant number ORF-2026-R478.

Institutional Review Board Statement: This study was approved by the Institutional Review Board of King Saud University (IRB number: E-24-9022, approval date: 12 September 2024).

Informed Consent Statement: According to the institution's Research Ethics Committee guidelines, the requirement for informed consent is waived provided that appropriate safeguards for privacy, confidentiality, and participants' rights are maintained. The research involved the use of dentin discs prepared from previously extracted human teeth, rather than direct experimentation on human participants. The dentin discs were obtained as residual biological material following clinical procedures and were appropriately anonymized.

Data Availability Statement: The original contributions presented in this study are included in the article/Supplementary Material. Further inquiries can be directed to the corresponding author.

Conflicts of Interest: The authors declare no conflicts of interest.

References

1. Siqueira, J.F., Jr.; Rôças, I.N.; Favieri, A.; Lima, K.C. Chemomechanical reduction of the bacterial population in the root canal after instrumentation and irrigation with 1%, 2.5%, and 5.25% sodium hypochlorite. *J. Endod.* **2000**, *26*, 331–334. [CrossRef] [PubMed]
2. Nair, P.N. Pathogenesis of apical periodontitis and the causes of endodontic failures. *Crit. Rev. Oral Biol. Med.* **2004**, *15*, 348–381. [CrossRef] [PubMed]
3. Gomes, B.P.; Bronzato, J.D.; Almeida-Gomes, R.F.; Pinheiro, E.T.; Sousa, E.L.R.; Jacinto, R.C. Identification of Fusobacterium nucleatum in primary and secondary endodontic infections and its association with clinical features by using two different methods. *Clin. Oral Investig.* **2021**, *25*, 6249–6258. [CrossRef] [PubMed]
4. Chen, Y.; Huang, Z.; Tang, Z.; Huang, Y.; Huang, M.; Liu, H.; Ziebolz, D.; Schmalz, G.; Jia, B.; Zhao, J. More Than Just a Periodontal Pathogen—The Research Progress on Fusobacterium nucleatum. *Front. Cell. Infect. Microbiol.* **2022**, *12*, 815318. [CrossRef] [PubMed]
5. Mohammadi, Z.; Dummer, P.M.H. Properties and applications of calcium hydroxide in endodontics and dental traumatology. *Int. Endod. J.* **2011**, *44*, 697–730. [CrossRef] [PubMed]
6. Chowdhury, K.; Antony, S.D.P.; Solete, P.; Elango, P.K.; Sanghavi, A.; Muskan, S. Effectiveness of calcium hydroxide as an intracanal medicament in endodontic retreatment: A systematic review of clinical outcome. *J. Conserv. Dent. Endod.* **2025**, *28*, 849–858. [CrossRef] [PubMed]
7. Ordinola-Zapata, R.; Noblett, W.C.; Perez-Ron, A.; Ye, Z.; Vera, J. Present status and future directions of intracanal medicaments. *Int. Endod. J.* **2022**, *55*, 613–636. [CrossRef] [PubMed]
8. Yarahmadi, A.; Dousti, B.; Karami-Khorramabadi, M.; Afkhami, H. Materials based on biodegradable polymers chitosan/gelatin: A review of potential applications. *Front. Bioeng. Biotechnol.* **2024**, *12*, 1397668. [CrossRef] [PubMed]
9. Farhadian, N.; Godiny, M.; Moradi, S.; Azandaryani, A.H.; Shahlaei, M. Chitosan/gelatin as a new nano-carrier system for calcium hydroxide delivery in endodontic applications: Development, characterization and process optimization. *Mater. Sci. Eng. C* **2018**, *92*, 540–546. [CrossRef] [PubMed]
10. Thein-Han, W.W.; Saikhun, J.; Pholpramoo, C.; Misra, R.; Kitiyanant, Y. Chitosan-gelatin scaffolds for tissue engineering: Physico-chemical properties and biological response of buffalo embryonic stem cells and transfectant of GFP-buffalo embryonic stem cells. *Acta Biomater.* **2009**, *5*, 3453–3466. [CrossRef] [PubMed]
11. Ferreira, N.S.; Martinho, F.C.; Cardoso, F.G.; Nascimento, G.G.; Carvalho, C.A.; Valera, M.C. Microbiological profile resistant to different intracanal medications in primary endodontic infections. *J. Endod.* **2015**, *41*, 824–830. [CrossRef] [PubMed]
12. Muchova, M.; Balacco, D.L.; Grant, M.M.; Chapple, I.L.C.; Kuehne, S.A.; Hirschfeld, J. Fusobacterium nucleatum subspecies differ in biofilm forming ability in vitro. *Front. Oral Health* **2022**, *3*, 853618. [CrossRef] [PubMed]
13. O'Toole, G.A.; Kolter, R. Initiation of biofilm formation in Pseudomonas fluorescens WCS365 proceeds via multiple, convergent signalling pathways: A genetic analysis. *Mol. Microbiol.* **1998**, *28*, 449–461. [CrossRef] [PubMed]

14. Abdallah, B.M.; Haack-Sørensen, M.; Burns, J.S.; Elsnab, B.; Jakob, F.; Hokland, P.; Kassem, M. Maintenance of differentiation potential of human bone marrow mesenchymal stem cells immortalized by human telomerase reverse transcriptase gene despite of extensive proliferation. *Biochem. Biophys. Res. Commun.* **2005**, *326*, 527–538. Erratum in *Biochem. Biophys. Res. Commun.* **2005**, *329*, 1361. [CrossRef] [PubMed]
15. Simonsen, J.L.; Rosada, C.; Serakinci, N.; Justesen, J.; Stenderup, K.; Rattan, S.I.; Jensen, T.G.; Kassem, M. Telomerase expression extends the proliferative life-span and maintains the osteogenic potential of human bone marrow stromal cells. *Nat. Biotechnol.* **2002**, *20*, 592–596. [CrossRef] [PubMed]
16. Gruber, S.; Nickel, A. Toxic or not toxic? The specifications of the standard ISO 10993-5 are not explicit enough to yield comparable results in the cytotoxicity assessment of an identical medical device. *Front. Med. Technol.* **2023**, *5*, 1195529. [CrossRef] [PubMed]
17. Mi, F.L. Synthesis and characterization of a novel chitosan-gelatin bioconjugate with fluorescence emission. *Biomacromolecules* **2005**, *6*, 975–987. [CrossRef] [PubMed]
18. Rinaudo, M. Chitin and chitosan: Properties and applications. *Prog. Polym. Sci.* **2006**, *31*, 603–632. [CrossRef]
19. Roig, X.; Halbaut, L.; Elmsmari, F.; Pareja, R.; Arrien, A.; Duran-Sindreu, F.; Delgado, L.M.; Espina, M.; García, M.L.; Sánchez, J.A.G.; et al. Calcium hydroxide-loaded nanoparticles dispersed in thermosensitive gel as a novel intracanal medicament. *Int. Endod. J.* **2024**, *57*, 907–921. [CrossRef] [PubMed]
20. Farhadian, N.; Godiny, M.; Mansouri, A.; Moradi, S.; Tajehmiri, A.; Shahlaei, M. Hydrophilic natural polymers for sustained-controlled release of calcium hydroxide. *Iran. J. Pharm. Res. IJPR* **2020**, *19*, 323–332. [CrossRef] [PubMed]
21. Heng, P.W. Controlled release drug delivery systems. *Pharm. Dev. Technol.* **2018**, *23*, 833. [CrossRef] [PubMed]
22. Shrestha, P.A.; Kishen, P.A. Antibacterial nanoparticles in endodontics: A review. *J. Endod.* **2016**, *42*, 1417–1426. [CrossRef] [PubMed]
23. Rabea, E.I.; Badawy, M.E.; Stevens, C.V.; Smagghe, G.; Steurbaut, W. Chitosan as antimicrobial agent: Applications and mode of action. *Biomacromolecules* **2003**, *4*, 1457–1465. [CrossRef] [PubMed]
24. Portenier, I.; Haapasalo, H.; Rye, A.; Waltimo, T.; Ørstavik, D.; Haapasalo, M. Inactivation of root canal medicaments by dentine, hydroxylapatite and bovine serum albumin. *Int. Endod. J.* **2001**, *34*, 184–188. [CrossRef] [PubMed]
25. Elmsmari, F.; Sánchez, J.A.G.; Duran-Sindreu, F.; Belkadi, R.; Espina, M.; García, M.L.; Sánchez-López, E. Calcium hydroxide-loaded PLGA biodegradable nanoparticles as an intracanal medicament. *Int. Endod. J.* **2021**, *54*, 2086–2098. [CrossRef] [PubMed]
26. Endytiastuti, E.; Ardhani, R.; Pidhatika, B.; Swasono, Y.A.; Rudianto, R.P.; Handajani, J.; Al-qatta, G.A.; Sudarso, I.S.R.; Busra, F.M. Gelatin/chitosan delivery system improves stability and regenerative potential of $Ca(OH)_2$ in an open dental pulp model. *BMT* **2025**. [CrossRef]
27. Li, X.; Han, B.; Wang, X.; Gao, X.; Liang, F.; Qu, X.; Yang, Z. Chitosan-decorated calcium hydroxide microcapsules with pH-triggered release for endodontic applications. *J. Mater. Chem. B* **2015**, *3*, 8884–8891. [CrossRef] [PubMed]
28. Ruparel, N.B.; Teixeira, F.B.; Ferraz, C.C.; Diogenes, A. Direct effect of intracanal medicaments on survival of stem cells of the apical papilla. *J. Endod.* **2012**, *38*, 1372–1375. [CrossRef] [PubMed]
29. Trevino, E.G.; Patwardhan, A.N.; Henry, M.A.; Perry, G.; Dybdal-Hargreaves, N.; Hargreaves, K.M.; Diogenes, A. Effect of irrigants on the survival of human stem cells of the apical papilla in a platelet-rich plasma scaffold in human root tips. *J. Endod.* **2011**, *37*, 1109–1115. [CrossRef] [PubMed]

Disclaimer/Publisher's Note: The statements, opinions and data contained in all publications are solely those of the individual author(s) and contributor(s) and not of MDPI and/or the editor(s). MDPI and/or the editor(s) disclaim responsibility for any injury to people or property resulting from any ideas, methods, instructions or products referred to in the content.